# Delayed collapses of BECs in relation to AdS gravity

Anxo F. Biasi[1], Javier Mas[1] and Angel Paredes[2]
[1] *Departamento de Física de Partículas, Universidade de Santiago de Compostela and Instituto Galego de Física de Altas Enerxías (IGFAE), E-15782, Santiago de Compostela, Spain.*
[2] *Departamento de Física Aplicada, Universidade de Vigo, As Lagoas s/n, Ourense, E-32004 Spain.*

We numerically investigate spherically symmetric collapses in the Gross-Pitaevskii equation with attractive nonlinearity in a harmonic potential. Even below threshold for direct collapse, the wave function bounces off from the origin and may eventually become singular after a number of oscillations in the trapping potential. This is reminiscent of the evolution of Einstein gravity sourced by a scalar field in Anti-de Sitter space where collapse corresponds to black hole formation. We carefully examine the long time evolution of the wave function for continuous families of initial states in order to sharpen out this coincidence which may bring new insights in both directions. On one hand, we comment on possible implications for the so-called Bosenova collapses in cold atom Bose-Einstein condensates. On the other hand, Gross-Pitaevskii provides a toy model to study the relevance of either the resonance conditions or the nonlinearity for the problem of Anti-de Sitter instability.

PACS numbers: 05.45.-a, 03.75.Kk, 04.25.dc

arXiv:1610.04866v2 [nlin.PS] 4 Nov 2016

## I. INTRODUCTION

The nonlinear Schrödinger equation (NLSE), sometimes called Gross-Pitaevskii equation (GPE) is a paradigmatic model for nonlinear systems. Different versions have been used in diverse contexts including, *e.g.* optics [1, 2], plasma physics [3] and even in cosmology [4, 5]. It describes with precision most of the physics of Bose-Einstein condensed (BEC) dilute gases [6, 7]. With an attractive nonlinearity, the wavefunction can self-focus and collapse, diverging at some point of space in finite time [8]. This can happen in cold atom BECs when the scattering length $a$ controlling the effective atom-atom interaction is negative [9–11]. The phenomenon, sometimes nicknamed "Bosenova" because of the subsequent explosion, has been demonstrated in a series of experiments which have attained a notable degree of control [12–15] and modeled using GPE [16–20].

There is a vast literature on collapses in GPE/NLSE, comprising analytic results, numerics and experiments [8, 21, 22]. Altogether, the standard lore is that collapse happens as soon as some parameter of the initial state, for example the overall energy or the peak value, surpasses some threshold. Near collapse, solutions typically display self-similarities [8, 23].

In a totally different arena, collapses have also been studied in general relativity (GR), in relation to black hole (BH) formation. In asymptotically flat space, a critical value for a given parameter marks the limit between collapse and dispersion to infinity of the initial matter distribution [24]. Remarkably, solutions at threshold also display extremely interesting self-similarities both of discrete and continuous type [25, 26].

In recent times, a modified version of this gravitational phenomenology has been explored in Anti de Sitter (AdS), the maximally symmetric spacetime with negative curvature. The most dramatic difference is that space becomes effectively bounded. Initial conditions that do not form a BH right away, reach the boundary and bounce, falling back again towards the origin with a different radial profile. The surprising result of [27] is that, no matter how small the initial amplitude, collapse eventually happens after a number of bounces of the matter field against the boundary. The initial claim was that the underlying mechanism is an energy cascade triggered by a fully resonant spectrum of the linearized perturbations. Later, the picture has proved to be more intricate and has thereby become a subject of intense research.

It seems natural to look for analogue features in other nonlinear systems. In this work, we have set up an efficient numerical code for radially symmetric long time simulations of the GPE. In order to reproduce features of the scalar field in AdS, we consider a quadratic potential, whose spectrum is fully resonant. Moreover, this potential typically models BEC traps and thus the framework is closely related to Bosenovae. Mathematical properties of the GPE in a harmonic trap has been studied elsewhere [28–30]. Our setup is similar in spirit to the evolution of a probe scalar in AdS [31].

We perform series simulations with decreasing initial amplitude in different number of dimensions $d$. Below threshold for direct collapse, a singularity is reached after a number of oscillations. We refer to these as "delayed collapses" following the nomenclature from the GR context [32]. We see a stepwise structure of delayed collapses. In the physical $d = 3$ case, our plots resemble those of wide initial gaussians in AdS [33], or those of theories with a mass gap for BH formation, such as $AdS_3$ [34], Einstein-Maxwell-scalar [35] or Einstein-Gauss-Bonnet [36, 37]. There are plateaux for which collapses occur after a number of bounces and transition regions where the collapsing time becomes a chaotic function of the initial amplitude. Below some amplitude, we do not find collapse in computational time. In $d = 7$,

our results become surprisingly similar to those of [27].

## II. FORMALISM

The wavefunction $\psi(t,r)$, evolving in a $d$-dimensional harmonic isotropic trap $V(r)=\frac{r^2}{2}$ with cubic focusing nonlinearity, is governed by

$$i\partial_t\psi = -\frac{1}{2}\partial_r^2\psi - \frac{d-1}{2r}\partial_r\psi + \frac{1}{2}r^2\psi - |\psi|^2\psi\,. \quad (1)$$

Without loss of generality, we use dimensionless quantities and give in the appendix the well-known rescaling from the dimensionful BEC variables. The norm and hamiltonian are conserved

$$N = S_d\int_0^\infty r^{d-1}|\psi|^2 dr\,, \quad (2)$$

$$H = \frac{S_d}{2}\int_0^\infty r^{d-1}\left(\partial_r\psi^*\partial_r\psi + r^2|\psi|^2 - |\psi|^4\right)dr\,, \quad (3)$$

where $S_d$ is the integral over the angles, *e.g.* $S_2=2\pi$, $S_3=4\pi$. An important indicator is the variance $V = S_d\int_0^\infty r^{d+1}|\psi|^2 dr$. $V=0$ implies collapse, but collapses can occur with $V\neq 0$. A straightforward calculation shows that $V$ satisfies the virial identity

$$\frac{d^2V}{dt^2} = 4H - 4V - (d-2)S_d\int_0^\infty r^{d-1}|\psi|^4 dr\,. \quad (4)$$

In order to connect the setup to weak turbulence [38, 39], the evolution equation can be rewritten in terms of modes by taking

$$\psi(t,r) = \sum_{n=0}^{\infty}\alpha_n(t)e^{-i\,\mu_n^{(d)}t}f_n^{(d)}(r) \quad (5)$$

where the $f_n^{(d)}(r)$ are the orthonormal basis of eigenfunctions of the linear problem (see appendix). We now insert (5) in (1), project on the $f_n^{(d)}(r)$ and assume that the rate of change of the $\alpha_n$ is much lower than that of the complex exponentials. This multiscale analysis is standard and goes under different names: rotating wave approximation, two-time formalism [40], averaging [41], etc. We find

$$\dot\alpha_l(t) = i\sum_{i=0}^{\infty}\sum_{j=0}^{\infty}\sum_{k=0}^{\infty}C_{ijkl}\alpha_i(t)\alpha_j(t)\alpha_k^*(t)\,, \quad (6)$$

where

$$C_{ijkl} = \delta_{i+j,k+l}S_d\int r^{d-1}f_i^{(d)}(r)f_j^{(d)}(r)f_k^{(d)}(r)f_l^{(d)}(r)dr\,. \quad (7)$$

The two conserved quantities (2), (3) (as in [31]) and the coincidence of the only resonant channel, $i+j=k+l$, relate closely the GPE formalism to the AdS setup [42, 43], and imply the coexistence of direct and inverse energy cascades.

An important ingredient is the family of initial conditions. We use gaussians of width $\sigma$ and amplitude $\epsilon$

$$\psi(t=0,r) = \epsilon\, e^{-r^2/\sigma^2}\,. \quad (8)$$

The choice is motivated by simplicity and the discussion is not significantly affected by this particular shape. Eq. (8) gives the ground state of the linear problem in which the harmonic potential has an extra $4\sigma^{-4}$ factor. Hence one can think of the processes we simulate as quenches in which at $t=0$ the linear and/or nonlinear potentials are abruptly modified initiating the dynamical evolution. In BECs, this is accomplished by tuning external fields which not only constitute the harmonic trap but do severely affect the atom-atom scattering length near Feshbach resonances [44].

## III. NUMERICAL ANALYSIS

Our work relies on numerical integration of Eq. (1). The reader interested in the methods can find all the details in the appendix. We start by briefly commenting on $d=2$. In BECs, this limit is achieved with a strongly anisotropic trap leading to a disk-shaped condensate [45]. In the absence of external potential, the Townes profile [46, 47] marks the limit between directly collapsing waves and those dispersing to infinity. The harmonic potential changes the picture, permitting stable stationary solutions [48]. We have not found any set of initial conditions yielding the sought structure of delayed collapses and below threshold solutions remain regular for all times.

In $d=3$ without trapping potential, there is also a sharp separation between direct collapse and dispersion. With a harmonic potential, apart from having periodic stationary solutions [49, 50], delayed collapses are possible. Figure 1 shows several examples in which a divergence of $\psi(t=t_c,r=0)$ is reached after several oscillations. This number of oscillations can be adjusted by fine-tuning the initial conditions.

In figure 2, we plot the time of collapse, $t_c$, as a function of $\epsilon$ for fixed $\sigma^2=1/2$. In the cold atom framework, tuning $\epsilon$ is equivalent to tuning the scattering length. Thus, this plot depicts the same observable as, *e.g.*, Fig. 2 of [14].

There are three distinct regions. For large $\epsilon$ there is direct collapse and $t_c$ decreases with growing $\epsilon$. For small $\epsilon$ solutions stay regular within computational time. There is a noteworthy intermediate transition region where some step structure is apparent (cf. Fig. 2). Roughly speaking, each step corresponds to a number of bounces in the harmonic potential. At the boundary between steps, $t_c$ has a bump. Our plot shows remarkable features in common with those found in different AdS setups (cf.

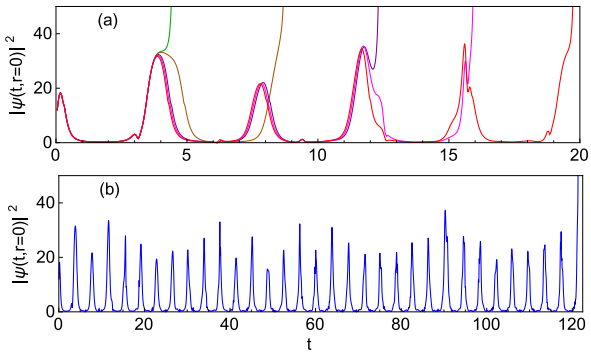


FIG. 1. Examples of delayed collapses in $d = 3$. We depict the value of $|\psi(t, r = 0)|^2$ for $\sigma^2 = 2/5$ and varying $\epsilon$. In each case, the wavefunction promptly collapses after hitting the upper limit of the plot. In panel (a), ordered by growing $t_c$, we have $\epsilon = 3.1286, 3.1285, 3.1280, 3.1277, 3.1273$. Notice the approximate overlap for long ranges of $t$. In panel (b), $\epsilon = 3.1270$ results in collapse after many bounces.

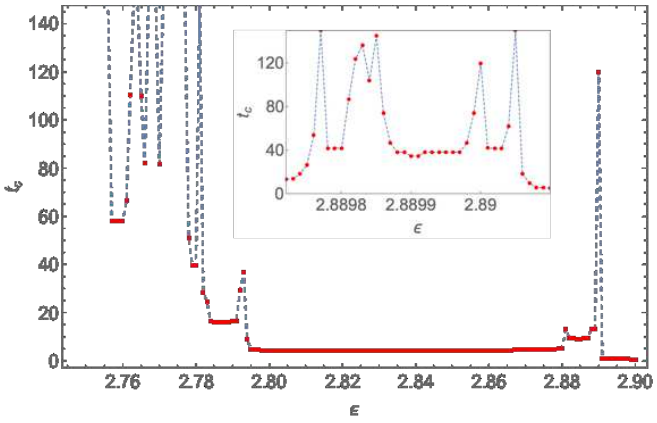


FIG. 2. Time of collapse for a family of initial conditions with $\sigma^2 = 1/2$ in $d = 3$. Prompt collapse occurs for $\epsilon > 2.891$. The resolution of the peak at the transition $\epsilon \sim 2.889$ exhibits a chaotic structure (in the inset).

Figs. 9 in [33], 3 in [51], 16 in [35] or 2 in [36]). The chaotic character of the curve at the bumps has been recently established in [37]. The common feature of these examples seems to be the lack of fully resonant linearized perturbations around a standing wave [52].

Figure 3 depicts a map of the results obtained with different $\epsilon$ and $\sigma$. The transition line between prompt and delayed collapse can be defined with precision. On the other hand, regularity of evolution can only be stated within a given computational time, which we have fixed to $t = 100$. The delayed collapse window is certainly narrow in the two-parameter space of initial conditions.

As mentioned above, our interest in looking for delayed collapses in GPE was sparked by the similar problem in the gravitational context of a scalar field coupled to

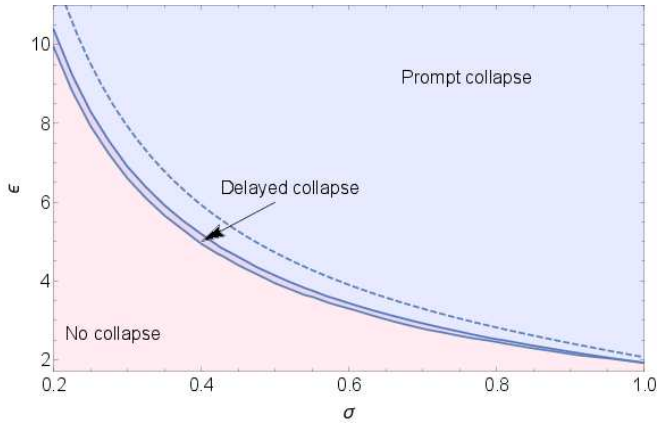


FIG. 3. Sectors for prompt and delayed collapse in $d = 3$. The dashed line signals the transition from initial conditions where $d^2V/dt^2|_{t=0}$ changes from negative (above) to positive (below). All delayed collapses happen with $V \neq 0$.

gravity and a negative cosmological constant. Now we can reverse the lore, and ask ourselves what we can learn from this nonlinear system in regard to the important question of the instability of AdS. In fact, one advantage of this simple equation is the fact that we can tweak separate features independently, like the property of full resonance or the character of the nonlinearity. These features are utterly mixed in the gravitational setup and are difficult to disentangle [53].

There is growing consensus that the weak turbulent instability of AdS, *i.e.*, that initial data always collapse in the limit $\epsilon \to 0$, is not solely caused by a fully resonant spectrum. This being a necessary condition, needs to be supplemented with appropriate asymptotics for the coupling coefficients $C_{ijkl}$ (7) at large values of $i, j, k, l \to \infty$ in a resonant channel. This should trigger efficient energy transfer to the high frequency modes. In the three-dimensional GPE, we have checked that $C_{in,jn,kn,ln}$ behaves with $n \to \infty$ as a power $n^\gamma$ with $\gamma = -0.5$. This is substantially lower a growth than the one observed in $AdS_4$ where $\gamma = 1$ in this channel [54] (in order to compare the resonant system in AdS with ours in Eq. (6), the modes $\alpha_i$ need to be rescaled to $\alpha_i/\sqrt{\omega_i}$. This shifts $\gamma = d \to d - 2$).

A natural question is what minimal twist could we perform in order to enhance the asymptotics, and whether this would have the expected impact on the collapse at low values of the initial amplitude. One possibility is to include derivative terms, (derivative couplings appear in the effective equations for a scalar field coupled to gravity). In fact, a term of the form $|\partial_r\psi|^2\psi$ added to the GPE yields $\gamma \approx 0.5$. The numerical evolution of the system with this additional term becomes unstable and we have deferred its study.

Another artificial but efficient way to enhance $\gamma$ is to

formally extend the GPE to higher dimensions. In figure 4, we depict the behavior of $C_{nnnn}$ for $n \leq 300$ and $d = 2, \ldots, 7$. In the large $n$ limit the exponent $\gamma$ behaves with the dimension as (see the appendix)

$$\gamma = \frac{d}{2} - 2, \tag{9}$$

a fact that presumably causes the different qualitative behavior between $d = 2$ and $d = 3$. This suggests that turbulence and collapse are favored at large $d$. This expectation is borne out by the results of figure 5, which shows a neat step structure for $t_c(\epsilon)$ when $d = 7$, resembling $AdS_4$ [27]. We also display the results with a slightly modified potential $V(r) = \frac{1}{2}r^\alpha$, where $\alpha = 2$ corresponds to the harmonic case. Changing $\alpha$ modifies the eigenvalues of the linear problem, breaking full resonance. As shown in fig. 5 this has a dramatic impact on the time of collapse at low initial amplitudes.

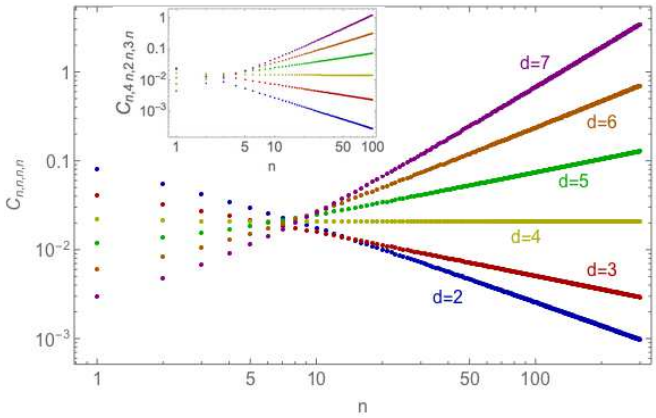


FIG. 4. Doubly logarithmic plot of $C_{nnnn}$ as a function of $n$ for different values of $d$. In the inset, we depict the $C_{n,4n,2n,3n}$, showing that they present a similar behavior.

## IV. DISCUSSION

Collapses in GPE/NLSE have been thoroughly studied but are still a fascinating topic. We have studied the long time evolution of the wave function in a trap, modeled by a harmonic potential. In $d = 3$, we have seen that there are initial conditions that lead to delayed collapses, where the divergence occurs after a number of oscillations. On average, the time of collapse grows with the inverse of the norm of the initial wavefunction, but non-monotonically and with a strong sensitivity to the initial condition. This happens in a region of parameter space which separates direct collapse from absence of collapse. Natural questions are how generic this behavior is and under which circumstances it can appear.

One intriguing answer is given by comparing to a scalar field in AdS gravity which shows remarkable similarities.

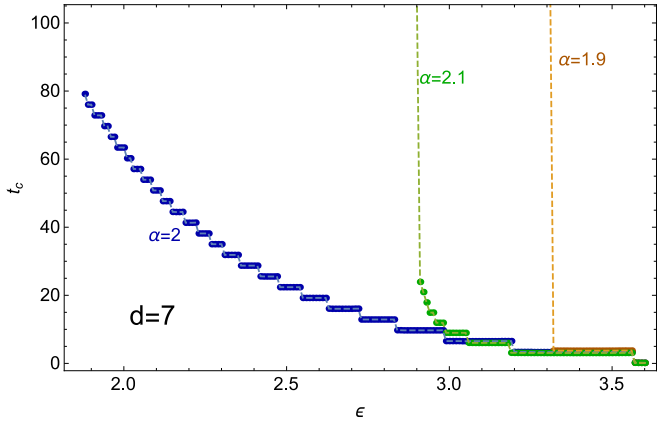


FIG. 5. Curve of $t_c$ vs. $\epsilon$ for $d = 7$ with $\sigma^2 = \frac{1}{2}$ and $V(r) = \frac{1}{2}r^\alpha$. Two non-resonant cases $\alpha = 1.9$ and $\alpha = 2.1$ present limiting values of $\epsilon$ below which no singularity is reached in computational time. The harmonic resonant case $\alpha = 2$ (Eq. (1)) shows a regularly spaced set of steps extending to much lower values of $\epsilon$.

The GPE evolution equations are much simpler than those of AdS gravity, and their study might be instrumental in understanding which peculiarities of general relativity are essential for the delayed collapse behavior and which are shared by other kinds of nonlinear systems. For instance, the behavior of the $C_{ijkl}$ coefficients (7) can be tuned by considering larger dimensions, nontrivial spatial profiles for the nonlinear coupling or other generalizations of Eq. (1). Studying the $d = 7$ case, we have shown that turbulence is enhanced by the rapidly growing $C_{ijkl}$ and that breaking the full resonance by tuning the potential sharply affects the long time evolution.

The GPE/NLSE is an ubiquitous formalism in nonlinear waves, and this fact can pave the way for tabletop experiments with analogies to AdS gravity. The experimental control reached in BECs might provide an ideal framework to realize the delayed collapse phenomenology. Our formalism is not a complete description of any such system since, for instance, it does not include anisotropies or losses by three-body recombinations. However, our results suggest that it might be worth revisiting, theoretically and/or experimentally, the transition from a stable BEC with attractive nonlinearity to a Bosenova collapse (cf. Fig. 2 of [14]). Depending on the width of the initial wavefunction, $t_c$ can decrease with the strength of the interaction $|a|$, a counterintuitive behavior. Moreover, there are narrow regions of parameter space where $t_c$ changes chaotically. Whether these properties stemming from Eq. (1) can be consequential in a realistic setup is a challenging question for the future.

## APPENDIX

In this appendix we lay out some technicalities related to the main text. First, in order to be reasonably self-contained, we write down some useful well-known equations concerning the rescaling of Gross-Pitaevskii equations (GPE) and the radially symmetric eigenmodes of a harmonic potential in $d \geq 2$ dimensions. Then, we specify some details regarding the employed numerical methods and cross-checks.

### GPE in adimensional form

The Gross-Pitaevskii mean-field description of a dilute Bose-Einstein condensate of bosons of mass $m$ in an isotropic harmonic potential of frequency $\omega$ is:

$$i\hbar\partial_{\tilde{t}}\tilde{\psi} = -\frac{\hbar^2}{2m}\tilde{\nabla}^2\tilde{\psi} + \frac{m\omega^2}{2}\tilde{r}^2\tilde{\psi} + \frac{4\pi\hbar^2 a}{m}|\tilde{\psi}|^2\tilde{\psi} \qquad (10)$$

where $a$ is the s-wave scattering length which can be positive (repulsive interaction) or negative (attractive interaction) and $\tilde{N} = \int |\tilde{\psi}|^2 d^3\tilde{\mathbf{r}}$ is the number of bosons in the sample. Tilded symbols represent physical quantities as opposed to the dimensionless ones of the main text. The relation between them is given by:

$$\frac{\tilde{t}}{t} = \omega^{-1}, \qquad \frac{\tilde{r}}{r} = \sqrt{\frac{\hbar}{m\omega}}, \qquad \frac{\tilde{\psi}}{\psi} = \sqrt{\frac{m\omega}{4\pi\hbar|a|}}\,. \qquad (11)$$

Inserting these expressions in (10), taking $a < 0$ and assuming that $\psi$ only depends on $t$ and $r$ we get the differential equation studied in the main text. It is immediate to compute the relation between the normalization of both conventions:

$$\tilde{N} = \frac{1}{4\pi|a|}\sqrt{\frac{\hbar}{m\omega}}N \qquad (12)$$

### Eigenfunctions of the harmonic oscillator

The angle-independent solutions of the linear harmonic oscillator problem:

$$i\partial_t\psi = -\frac{1}{2}\partial_r^2\psi - \frac{d-1}{2r}\partial_r\psi + \frac{1}{2}r^2\psi \qquad (13)$$

with $d \geq 2$ can be written as:

$$\psi = \sum_{n=0}^{\infty} \alpha_n e^{-i\mu_n^{(d)}t} f_n^{(d)}(r)\,. \qquad (14)$$

The eigenvalues are:

$$\mu_n^{(d)} = 2n + d/2 \qquad (15)$$

and the eigenfunctions take the form:

$$f_n^{(d)}(r) = \sqrt{\frac{n!\Gamma(\frac{d}{2})}{\pi^{d/2}\Gamma(\frac{d}{2}+n)}}\; L_n^{(d-2)/2}(r^2)e^{-r^2/2}\,. \qquad (16)$$

The $L_n^{(d-2)/2}$ are generalized Laguerre polynomials, $\Gamma$ represents Euler's gamma function and the multiplicative constant is chosen to satisfy the orthonormality condition:

$$S_d \int r^{d-1} f_m^{(d)} f_n^{(d)} dr = \delta_{mn} \qquad (17)$$

where:

$$S_d = \frac{\pi^{d/2} d}{\Gamma(\frac{d}{2}+1)}\,. \qquad (18)$$

The coefficient for a given mode is found by projecting the wavefunction onto the appropriate eigenfunction $|\alpha_n| = S_d|\int r^{d-1} f_n^{(d)}(r)\psi dr|$.

### Numerical details and quality checks

In the region of delayed collapses, small changes in initial conditions can lead to rather different results. Thus, a method for fast, stable and precise computation is needed and it is worth to briefly describe here the one we have used. Our integration algorithm relies on an explicit finite difference scheme consistent with fourth order accuracy and convergence. Spatial derivatives are discretized with standard stencils, and time evolution uses a fourth order Runge-Kutta. The Courant factor, $c$, depends on the discretization density since the equation is parabolic. Stability enforces this number to be quite small. For $2^w$ points in the spatial grid, we have used $c = 0.004 \times 2^{12-w}$ with $w = 12, ..., 17$.

At the origin, we ensure regularity by enforcing $\partial_r\psi(t, r = 0) = 0$. The harmonic potential confines the wavefunction and therefore $\psi$ decays exponentially with $r$. We have checked that choosing $r_{max} = 50$ keeps $\psi(r_{max}) \sim 10^{-15}$ so that setting its value to zero, and truncating $r$ to a finite interval $0 < r < r_{max}$, does not affect the simulation. We have also performed computations using a truly compact coordinate $r = z/(z_{max} - z)$ and found consistent results.

We have used the conservation of the norm (2), the hamiltonian (3), and the variance identity (4), as quality tests to monitor the computation. For initial conditions of the form (8), they take the values

$$N = \left(\frac{\pi}{2}\right)^{\frac{d}{2}} \epsilon^2\sigma^d\,,$$
$$H = \frac{d}{2}\left(\frac{\pi}{2}\right)^{\frac{d}{2}} \epsilon^2\sigma^d\left(\frac{1}{\sigma^2} + \frac{\sigma^2}{4} - \frac{\epsilon^2}{2^{\frac{d}{2}}d}\right)\,. \qquad (19)$$

The value of the second derivative of the variance at $t = 0$ is:

$$\left.\frac{d^2V}{dt^2}\right|_{t=0} = 2d\left(\frac{\pi}{2}\right)^{\frac{d}{2}}\epsilon^2\sigma^d\left(\frac{1}{\sigma^2} - \frac{\sigma^2}{4} - \frac{\epsilon^2}{2^{\frac{d}{2}+1}}\right). \quad (20)$$

We define the relative deviations $\delta N = \frac{N_{num}-N}{N}$, $\delta H = \frac{H_{num}-H}{H}$ where $N_{num}$, $H_{num}$ are the values obtained from numerical integration and $N$, $H$ are the values given in (19). To keep them satisfied at relative orders $\delta H, \delta N < 10^{-6}$ we have implemented global (in space) refinement. This is seen to be required when the profile becomes extremely sharp at the origin, and needs more resolution to keep numerical control. Fig. 6 depicts a check for one of the simulations yielding a delayed collapse.

We have implemented our codes for CPU computation and, in order to speed up the simulation, we also adapted them for GPGPU. The computation times that we achieve are approximately one order of magnitud lower in the latter case.

### Asymptotic values of the $C_{ijkl}$

We now obtain the asymptotically large $n$ behaviour of $C_{n(ijkl)}$. The form of the coefficients is given by the integral in (7) for the eigenfunctions of Eq. (16). We follow the procedure of [55]. Consider the identity [56]

$$L_n^{(\alpha)}(\nu x) \approx \frac{e^{\frac{1}{2}\nu x}}{2^\alpha x^{\frac{1}{2}\alpha+\frac{1}{4}}}\left(\xi^{1/2}J_\alpha(\nu\xi)\right) \quad (21)$$

valid in the limit $n \to \infty$, $x \ll 1$. $J_\alpha(x)$ are Bessel functions of the first kind and $\alpha = \frac{d}{2} - 1$, $\nu = 2\mu_n^{(d)}$, $\xi \approx \sqrt{x}$. Taking $r^2 = \nu x$, we get an expression for the eigenfunctions. Notice that the limit $x \ll 1$ is justified because $x = r^2/n$ with $n \to \infty$.

Now the Bessel functions are $J_\alpha(\nu^{1/2}r)$ and performing a change of variables in the integral (7), we can remove the dependence in $n$ from the argument. Using the asymptotic value for the normalization constants (cf. the prefactors in (16)) $N_n \sim n^{-\alpha/2}$, we obtain $C_{n(ijkl)} \sim n^{\frac{d}{2}-2}\int dz K(z)$ where $K(z)$ does not depend on $n$. Thus, we get equation (9).

We have checked that this expression is in agreement with the values of $C_{nnnn}$ and $C_{n,4n,2n,3n}$ found by numerical integration for $d = 2, \ldots, 7$, see figure 4.

*Acknowledgements.* We thank P. Carracedo, B. Craps, O. Evnin, A. Rostworowski and A. Serantes for useful comments. This work was supported by grants FPA2011-22594, FIS2014-58117-P and FIS2014-61984-EXP from Ministerio de Ciencia e Innovación and grants GPC2015/019, GRC2013/024, EM2013/002 and AGRUP2015/11 from Xunta de Galicia. Part of this research has benefited from the use computational resources/services provided by the Galician Supercomputing Centre (CESGA)

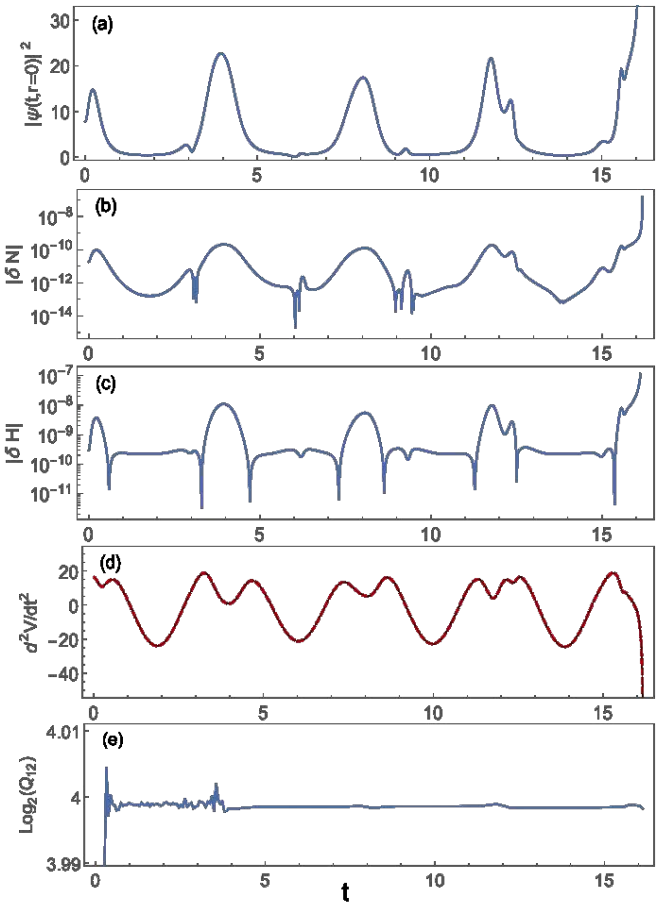


FIG. 6. A simulation with $d = 3$, $\epsilon = 2.79$ , $w = 14$, $\sigma^2 = 1/2$. Panel (a) represents $|\psi|^2$ at the origin. Panels (b) and (c) depict the relative deviations for the norm and hamiltonian, respectively. Panel (d) compares the second derivative of the variance from the numerical computation to that from the right-hand side of Eq. (4) computed at each step. Finally, panel (e) shows the convergence level along the whole simulation. On a grid of $2^w$ points, $Q_w = ||\psi_{w+1} - \psi_w||/||\psi_{w+2} - \psi_{w+1}||$ where $||\cdot||$ stands for a $L^2$ norm. The plot shows convergence at fourth order with high accuracy. The tests show that the numerical method is reliable until times very near collapse.

[1] G. P. Agrawal, *Nonlinear fiber optics*. Academic press (2007).
[2] B. A. Malomed, D. Mihalache, F. Wise, and L. Torner, "Spatiotemporal optical solitons," J. Opt. B: Quantum Semiclass. Opt. bf 7, R53, (2005).
[3] V. E. Zakharov, V. S. L'vov, and G. Falkovich, *Kolmogorov spectra of turbulence I: Wave turbulence.*

Springer Science & Business Media (2012).
[4] H.-Y. Schive, T. Chiueh, and T. Broadhurst, "Cosmic structure as the quantum interference of a coherent dark wave," Nat. Phys. **10**, 496 (2014).
[5] A. Paredes and H. Michinel, "Interference of dark matter solitons and galactic offsets," Phys. Dark Univ. **12**, 50 (2016).
[6] F. Dalfovo, S. Giorgini, L. P. Pitaevskii, and S. Stringari, "Theory of Bose-Einstein condensation in trapped gases," Rev. Mod. Phys. **71**, 463 (1999).
[7] R. Carretero-González, D. Frantzeskakis, and P. Kevrekidis, "Nonlinear waves in Bose–Einstein condensates: physical relevance and mathematical techniques," Nonlinearity **21**, R139 (2008).
[8] C. Sulem and P.-L. Sulem, *The nonlinear Schrödinger equation: self-focusing and wave collapse*, vol. 139. Springer Science & Business Media (2007).
[9] Y. Kagan, E. L. Surkov, and G. V. Shlyapnikov, "Evolution and global collapse of trapped Bose condensates under variations of the scattering length," Phys. Rev. Lett. **79**, 2604 (1997).
[10] Y. Kagan, A. E. Muryshev, and G. V. Shlyapnikov, "Collapse and Bose-Einstein condensation in a trapped Bose gas with negative scattering length," Phys. Rev. Lett. **81**, 933 (1998).
[11] L. Santos and G.V. Shlyapnikov, "Collapse dynamics of trapped Bose-Einstein condensates," Phys. Rev. A **66**, 011602 (2002).
[12] J. M. Gerton, D. Strekalov, I. Prodan, and R. G. Hulet, "Direct observation of growth and collapse of a Bose–Einstein condensate with attractive interactions," Nature, **408**, 692 (2000).
[13] J. L. Roberts, N. R. Claussen, S. L. Cornish, E. A. Donley, E. A. Cornell, and C. E. Wieman, "Controlled collapse of a Bose-Einstein condensate," Phys. Rev. Lett. **86**, 4211 (2001).
[14] E. A. Donley, N. R. Claussen, S. L. Cornish, J. L. Roberts, E. A. Cornell, and C. E. Wieman, "Dynamics of collapsing and exploding Bose–Einstein condensates," Nature **412**, 295 (2001).
[15] C. Eigen, A. L. Gaunt, A. Suleymanzade, N. Navon, Z. Hadzibabic, and R. P. Smith, "Observation of weak collapse in a Bose-Einstein condensate," *arXiv:1609.00352* (2016).
[16] H. Saito and M. Ueda, "Intermittent implosion and pattern formation of trapped Bose-Einstein condensates with an attractive interaction," Phys. Rev. Lett. **86**, 1406 (2001).
[17] H. Saito and M. Ueda, "Power laws and collapsing dynamics of a trapped Bose-Einstein condensate with attractive interactions," Phys. Rev. A **63**, 043601 (2001).
[18] S. K. Adhikari, "Mean-field description of collapsing and exploding Bose-Einstein condensates," Phys. Rev. A **66**, 013611 (2002).
[19] C.M. Savage, N.P. Robins, and J.J. Hope, "Bose-Einstein condensate collapse: A comparison between theory and experiment," Phys. Rev. A **67**, 014304 (2003).
[20] M. Ueda and H. Saito, "A consistent picture of a collapsing Bose–Einstein condensate," J. Phys. Soc. Jpn. **72**, 127 (2003).
[21] L. Bergé, "Wave collapse in physics: principles and applications to light and plasma waves," Phys. Rep. **303**, 259 (1998).
[22] G. Fibich, *The nonlinear Schrödinger equation*. Springer (2015).
[23] C. J. Budd, S. Chen, and R. D. Russell, "New self-similar solutions of the nonlinear Schrödinger equation with moving mesh computations," J. Comput. Phys. **152**, 756 (1999).
[24] D. Christodoulou, "The problem of a self-gravitating scalar field," Comm. Math. Phys. **105**, 337 (1986).
[25] M. W. Choptuik, "Universality and scaling in gravitational collapse of a massless scalar field," Phys. Rev. Lett. **70**, 9 (1993).
[26] C. Gundlach, "Critical phenomena in gravitational collapse," Phys. Rep. **376**, 339 (2003).
[27] P. Bizon and A. Rostworowski, "On weakly turbulent instability of anti-de Sitter space," Phys. Rev. Lett. **107**, 031102 (2011).
[28] R. Carles, "Remarks on nonlinear Schrödinger equations with harmonic potential," in *Annales Henri Poincaré*, vol. 3, pp. 757–772, Springer, 2002.
[29] C. Jao, "The energy-critical quantum harmonic oscillator," Comm. Partial Differential Equations, **41**, 79, (2016).
[30] Z. Hani and L. Thomann, "Asymptotic behavior of the nonlinear Schrödinger equation with harmonic trapping", Comm. Pure Appl. Math., 2015, Wiley Online Library.
[31] P. Basu, C. Krishnan, and A. Saurabh, "A stochasticity threshold in holography and the instability of AdS," Int. J. Mod. Phys. A **30**, 1550128 (2015).
[32] H. Okawa, V. Cardoso, and P. Pani, "Collapse of self-interacting fields in asymptotically flat spacetimes: do self-interactions render Minkowski spacetime unstable?," Phys. Rev. D **89**, 041502 (2014).
[33] A. Buchel, S. L. Liebling, and L. Lehner, "Boson stars in AdS spacetime," Phys. Rev. D **87**, 123006 (2013).
[34] E. da Silva, E. Lopez, J. Mas, and A. Serantes, "Holographic quenches with a gap," J. High Energy Phys **06**, 172 (2016).
[35] R. Arias, J. Mas, and A. Serantes, "Stability of charged global $AdS_4$ spacetimes," J. High Energy Phys. **09**, 024 (2016).
[36] N. Deppe, A. Kolly, A. Frey, and G. Kunstatter, "Stability of anti–de Sitter space in Einstein-Gauss-Bonnet gravity," Phys. Rev. Lett. **114**, 071102 (2015).
[37] N. Deppe, A. Kolly, A. R. Frey, and G. Kunstatter, "Black hole formation in AdS Einstein-Gauss-Bonnet gravity," *arXiv:1608.05402* (2016).
[38] G. Krstulovic and M. Brachet, "Dispersive bottleneck delaying thermalization of turbulent Bose-Einstein condensates," Phys. Rev. Lett. **106**, 115303, (2011).
[39] V. Shukla, M. Brachet, and R. Pandit, "Turbulence in the two-dimensional Fourier-truncated Gross–Pitaevskii equation," New J. Phys. **15**, 113025 (2013).
[40] V. Balasubramanian, A. Buchel, S. R. Green, L. Lehner and S. L. Liebling, "Holographic Thermalization, Stability of Anti-de Sitter Space, and the Fermi-Pasta-Ulam Paradox," Phys. Rev. Lett. **113**, no. 7, 071601 (2014).
[41] B. Craps, O. Evnin and J. Vanhoof, "Renormalization group, secular term resummation and AdS (in)stability," J. High Energy Phys. **10**, 048 (2014).
[42] B. Craps, O. Evnin, and J. Vanhoof, "Renormalization, averaging, conservation laws and AdS (in)stability," J. High Energy Phys. **01**, 108 (2015).
[43] A. Buchel, S. R. Green, L. Lehner, and S. L. Liebling, "Conserved quantities and dual turbulent cascades in anti-de Sitter spacetime," Phys. Rev. D **91**, 064026

(2015).

[44] C. Chin, R. Grimm, P. Julienne, and E. Tiesinga, "Feshbach resonances in ultracold gases," Rev. Mod. Phys. **82**, 1225 (2010).

[45] A. Görlitz, J.M. Vogels, A.E. Leanhardt, C. Raman, T.L. Gustavson, J.R. Abo-Shaeer, A.P. Chikkatur, S. Gupta, S. Inouye, T. Rosenband, and W. Ketterle "Realization of Bose-Einstein condensates in lower dimensions," Phys. Rev. Lett. **87**, 130402 (2001).

[46] R. Y. Chiao, E. Garmire, and C. H. Townes, "Self-trapping of optical beams," Phys. Rev. Lett. **13**, 479 (1964).

[47] K. D. Moll, A. L. Gaeta, and G. Fibich, "Self-similar optical wave collapse: Observation of the Townes profile," Phys. Rev. Lett. **90**, 203902, (2003).

[48] G. Herring, L.D. Carr, R. Carretero-González, P.G. Kevrekidis, and D.J. Frantzeskakis, "Radially symmetric nonlinear states of harmonically trapped Bose-Einstein condensates," Phys. Rev. A **77**, 023625 (2008).

[49] P. A. Ruprecht, M. J. Holland, K. Burnett, and M. Edwards, "Time-dependent solution of the nonlinear Schrödinger equation for Bose-condensed trapped neutral atoms," Phys. Rev. A **51**, 4704 (1995).

[50] K. Mallory and R. A. Van Gorder, "Stationary solutions for the nonlinear Schrödinger equation modeling three-dimensional spherical Bose-Einstein condensates in general potentials," Phys. Rev. E, **92**, 013201 (2015).

[51] V. Cardoso and J. V. Rocha, "Collapsing shells, critical phenomena, and black hole formation," Phys. Rev. D, **93**, 084034 (2016).

[52] M. Maliborski and A. Rostworowski, "What drives AdS spacetime unstable?," Phys. Rev. D **89**, 124006 (2014).

[53] R.-G. Cai, L.-W. Ji, and R.-Q. Yang, "Collapse of self-interacting scalar field in anti-de Sitter space," Commun. Theor. Phys. **65**, 329 (2016).

[54] B. Craps, O. Evnin and J. Vanhoof, "Ultraviolet asymptotics and singular dynamics of AdS perturbations," J. High Energy Phys. **10**, 079 (2015).

[55] O. Evnin and P. Jai-akson, "Detailed ultraviolet asymptotics for AdS scalar field perturbations," J. High Energy Phys. **04**, 054 (2016).

[56] NIST Digital Library of Mathematical Functions. http://dlmf.nist.gov/18.15, Release 1.0.13 of 2016-09-16. F. W. J. Olver, A. B. Olde Daalhuis, D. W. Lozier, B. I. Schneider, R. F. Boisvert, C. W. Clark, B. R. Miller, and B. V. Saunders, eds.